Chemical Constituents of the Deep-Sea-Derived Penicillium citrinum W17 and Their Anti-Inflammatory and Anti-Osteoporotic Bioactivities

Yong Zhang , Chun-Lan Xie , Yuan Wang , Xi-Wen He , Ming-Min Xie , You Li , Kai Zhang , Zheng-Biao Zou , Long-He Yang * , Xian-Wen Yang * , Ren Xu *

Posted Date: 25 September 2023

doi: 10.20944/preprints202309.1663.v1

Keywords: deep-sea; fungus; Penicillium citrinum; polyketides; anti-osteoporosis; anti-inflammation.

Article

Chemical Constituents of the Deep-Sea-Derived *Penicillium citrinum* W17 and Their Anti-Inflammatory and Anti-Osteoporotic Bioactivities

Yong Zhang [1,†], Chun-Lan Xie [1,2,†], Yuan Wang [1], Xi-Wen He [1], Ming-Min Xie [1], You Li [1], Kai Zhang [1], Zheng-Biao Zou [1], Long-He Yang [1,*], Ren Xu [2,*] and Xian-Wen Yang [1,*]

[1] Key Laboratory of Marine Genetic Resources, Technical Innovation Center for Utilization of Marine Biological Resources, Third Institute of Oceanography, Ministry of Natural Resources, 184 Daxue Road, Xiamen 361005, China

[2] School of Medicine, Xiamen University, South Xiangan Road, Xiamen 361005, China

* Correspondence: yangxianwen@tio.org.cn (X.-W.Y.); xuren526@xmu.edu.cn (R.X.); longheyang@tio.org.cn (L.Y.); Tel.: +86-592-219-5319 (X.-W.Y.); +86-592-288-0577 (R.X.); +86-592-219-5319 (L.Y.)

† These authors contributed equally to this work.

Abstract: Three new polyketides (penidihydrocitrinins A–C, **1–3**) and 14 known compounds (**4–17**) were isolated from the deep-sea-derived *Penicillium citrinum* W17. Their structures were elucidated by comprehensive analyses of 1D and 2D NMR, HRESIMS, and ECD calculations. Compounds **1–17** were evaluated for their anti-inflammatory and anti-osteoporotic bioactivities. All isolates exhibited significant inhibitory effects on microglial activation in LPS-stimulated BV-2 cells in a dose-response manner. Notably, compound **14** displayed the strongest effect with the IC_{50} value of 4.7 μM. Moreover, compounds **6**, **7**, and **8** not only suppressed osteoclastogenesis, but also promoted osteoblast mineralization.

Keywords: deep-sea; fungus; *Penicillium citrinum*; polyketides; anti-osteoporosis; anti-inflammation

1. Introduction

Marine microbes are an ideal source to yield diverse secondary metabolites with unprecedent structures. As a matter of fact, about half of the new marine natural products were produced by marine microorganisms [1–3], especially those living in the deep-sea under extreme tough environments such as low oxygen concentration, high salt, high hydrostatic pressure, and absence of light, which require various biochemical and physiological adaptations for survival [4,5]. These adaptions are accompanied by the adjustments of gene regulation, resulting in formation of different metabolic pathways to give birth to a large number of new secondary metabolites [4,5].

Polyketides are a class of structurally diverse natural products with the carbon skeletons originated from the polymerization of short-chain carboxylic acids units, including acetate, propionate, butyrate, etc [6]., which are catalyzed by polyketide synthases (PKS) [7]. Polyketides have attracted wide attention due to their promising bioactivities [8,9]. For example, salinosporamide A showed significant proteasomal chymotrypsin-like proteolytic inhibitory activity with an IC_{50} value of 1.3 nM [10]; microketide A exhibited remarkable antibacterial activities against *Pseudomonas aeruginosa*, *Nocardia brasiliensis*, *Kocuria rhizophila*, and *Bacillus anthraci* with an equal MIC value (0.19 μg/mL) as that of ciprofloxacin [11]; and theissenone exhibited potent nitric oxide production inhibitory activity in murine brain microglial BV-2 cells with IC_{50} value of 5.0 ± 1.0 μM [12]. As one of the most abundant fungi of the world, *Penicillium* species could generate a broad spectrum of unique polyketides. For instance, two new tricyclic polyketides, penijanthinones A and B, were isolated from *Penicillium janthinellum* HK1-6 [13,14]; two new C-8 benzoyl-substituted azaphilones, pinazaphilones A and B, were obtained from *Penicillium* sp. HN29-3B1 [13,14]; chloctanspirones A

Preprints (www.preprints.org) | NOT PEER-REVIEWED | Posted: 25 September 2023 doi:10.20944/preprints202309.1663.v1

and B, possessing an unprecedented bicyclo [2.2.2] octane-2-spiro cyclohexane skeleton, were discovered from *Penicillium terrestre* [15].

As part of our continuing discovery for structurally novel and biologically interesting compounds from deep-sea-derived microorganisms [16–20], *Penicillium citrinum* W17 isolated from a deep-sea sediment sample (−5278 m) of the Western Pacific Ocean was subjected to a systematically chemical investigation. As a result, three new polyketides (penidihydrocitrinins A–C, **1**–**3**) and 14 known compounds (**4**–**17**) were obtained (Figure 1). Herein, we report the details of isolation, structure elucidation, and bioactivities of these isolates.

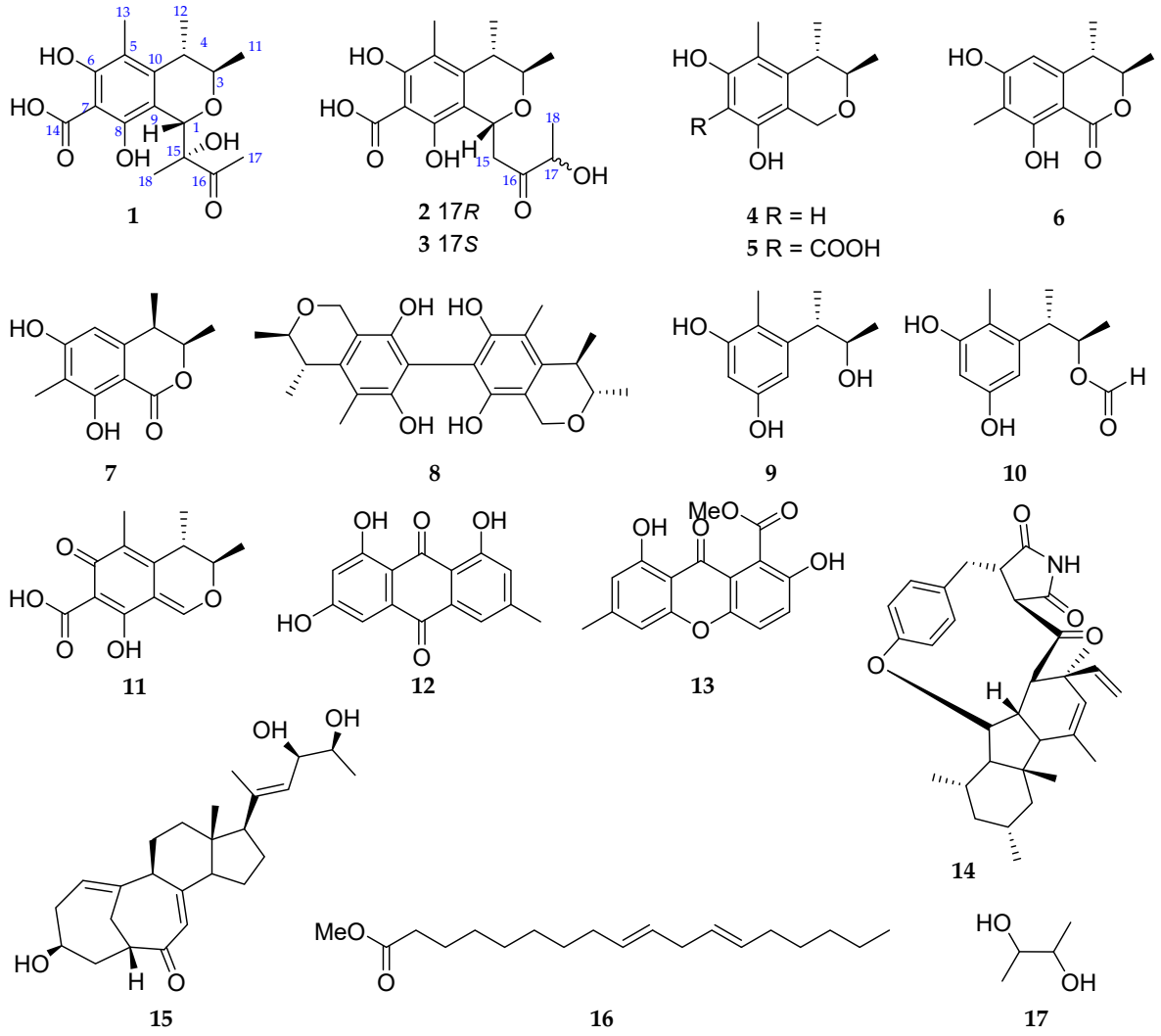

Figure 1. Compounds **1**–**17** isolated from *Penicillium citrinum* W17.

2. Results and Discussion

Compound **1** was obtained as yellow amorphous powder. The molecular formula was determined as $C_{17}H_{22}O_7$ with seven degrees of unsaturation (DoU) on the basis of HRESIMS data at *m*/*z* 337.1309 $[M - H]^-$. The ^1H NMR spectrum (Table 1) showed two methyl doublets [δ_H 1.11 (d, *J* = 6.4 Hz, 11-Me) and 1.28 (d, *J* = 6.9 Hz, 12-Me)], three methyl singlets [δ_H 1.10 (s, 18-Me), 2.04 (s, 13-Me), and 2.30 (s, 17-Me)], and three methines [δ_H 2.62 (qd, *J* = 6.7 Hz, 1.8 Hz, H-4), 3.98 (qd, *J* = 6.9 Hz, 1.8 Hz, H-3), 5.17 (s, H-1)]. The ^{13}C NMR spectroscopic data exhibited 17 carbon resonance signals, including five methyls [δ_C 10.2 (q, 13-Me), 18.3 (q, 11-Me), 20.1 (q, 12-Me), 20.7 (q, 18-Me), 25.0 (q, 17-Me)], three methines [(δ_C 36.9 (d, C-4), 74.0 (d, C-3), 75.4 (d, C-1)], and nine nonprotonated carbons [δ_C 83.2 (s, C-15), 102.2 (s, C-7), 110.3 (s, C-9), 114.0 (s, C-5), 143.8 (s, C-10), 156.7 (s, C-8), 160.0 (s, C-6), 178.2 (s, C-14), 211.3 (s, C-16)]. The COSY correlations of 11-Me/H-3/H-4/12-Me, together with the

Preprints (www.preprints.org) | NOT PEER-REVIEWED | Posted: 25 September 2023 doi:10.20944/preprints202309.1663.v1

HMBC correlations from H-4 to C-5 and C-10, from 13-Me to C-5, C-6, and C-10, from H-3 to C-10, and from H-1 to C-3, C-8, C-9, and C-10, constructed a dihydrocitrinin fragment. In combination with the HMBC cross peaks of 17-Me with C-16 and of 18-Me with C-1, C-15, and C-16, the planar structure of compound **1** was established as 2-hydroxy-3-butonyldihydrocitrinin (Figure 2).

Table 1. ^{1}H (400 Hz) and ^{13}C (100 Hz) NMR spectroscopic data of **1**–**3** (δ in ppm, J in Hz within parentheses).

No.	**1** [a]		**2** [b]		**3** [b]	
	δ_C	δ_H	δ_C	δ_H	δ_C	δ_H
1	75.4 CH	5.17 s	64.8 CH	5.08 (d, 9.7)	64.8 CH	5.08 (d, 9.2)
3	74.0 CH	3.98 (qd, 6.9, 1.8)	71.7 CH	3.82 (qd, 6.6, 1.5)	71.7 CH	3.82 (qd, 6.6, 1.5)
4	36.9 CH	2.62 (qd, 6.7, 1.8)	35.1 CH	2.52 m	35.2 CH	2.51 m
5	114.0 C		109.5 C		109.6 C	
6	160.0 C		158.5 C		158.5 C	
7	102.2 C		101.8 C		101.8 C	
8	156.7 C		155.8 C		155.8 C	
9	110.3 C		110.7 C		110.9 C	
10	143.8 C		139.7 C		139.8 C	
11	18.3 CH_3	1.11 (d, 6.4)	18.2 CH_3	1.01 (d, 6.5)	18.3 CH_3	0.99 (d, 6.5)
12	20.1 CH_3	1.28 (d, 6.9)	20.1 CH_3	1.17 (d, 6.8)	20.2 CH_3	1.17 (d, 7.2)
13	10.2 CH_3	2.04 s	9.5 CH_3	1.93 s	9.6 CH_3	1.92 s
14	178.2 C		175.6 C		175.7 C	
15	83.2 C		43.1 CH_2	2.66 m 3.23 m	43.0 CH_2	2.72 m 3.16 m
16	211.3 C		211.9 C		212.1 C	
17	25.0 CH_3	2.30 s	72.2 CH	4.11 m	72.8 CH	4.02 m
18	20.7 CH_3	1.10 s	19.2 CH_3	1.21 (d, 7.0)	19.0 CH_3	1.15 (d, 7.2)
6-OH				14.64 s		14.62 s
8-OH				15.16 s		15.13 s

[a] Recorded in CD_3OD. [b] Recorded in DMSO-d_6.

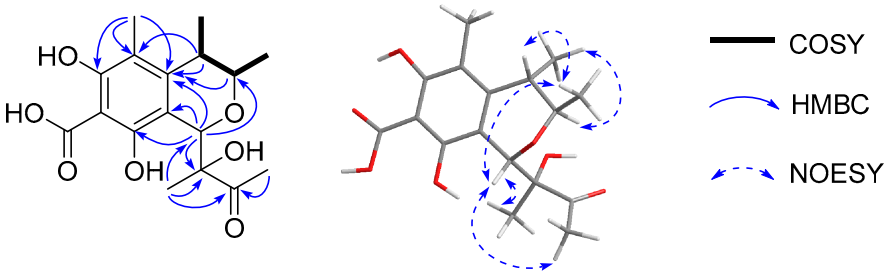

Figure 2. The key COSY, HMBC, and NOESY correlations of compound **1**.

The correlations of H-3/12-Me and11-Me/H-1/H-4 were observed in the NOESY spectrum, indicating H-1, H-4, and 11-Me were on the same plane, opposite to that of H-3 and 12-Me (Figure 3). Although the NOESY correlations were found of H-1 to 17-Me and 18-Me, revealing the relative configuration of C-15, more solid evidence should be needed to confirm the absolute configuration because of the flexible structure of the segment. Accordingly, the theoretical calculation of the electronic circular dichroism (ECD) spectrum of (1*S*,3*R*,4*S*,15*R*)-**1** and (1*S*,3*R*,4*S*,15*S*)-**1** were conducted along with their enantiomers of (1*R*,3*S*,4*R*,15*S*)-**1** and (1*R*,3*S*,4*R*,15*S*)-**1**. As shown in Figure 4, the calculated ECD spectrum of (1*S*,3*R*,4*S*,15*R*)-**1** matched well with that of the experimental

Preprints (www.preprints.org) | NOT PEER-REVIEWED | Posted: 25 September 2023 doi:10.20944/preprints202309.1663.v1

one. On the basis of the above evidences, compound **1** was determined as (1*S*,3*R*,4*S*,15*R*)-2-hydroxy-3-butonyldihydrocitrinin, and named penidihydrocitrinin A.

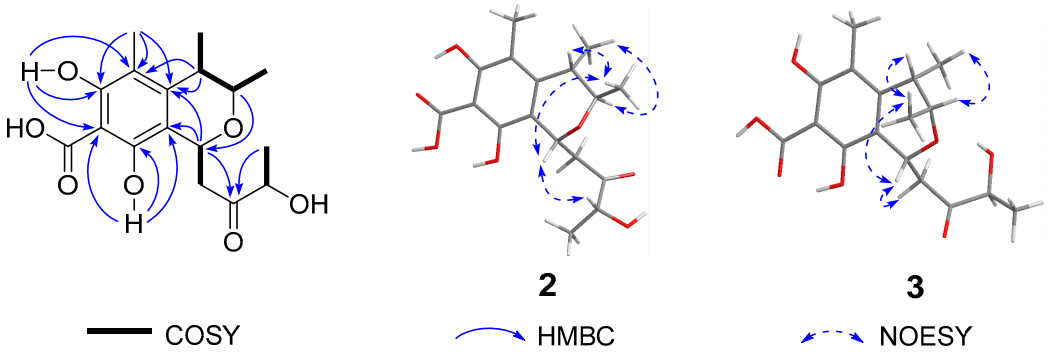

Figure 3. The key COSY, HMBC, and NOESY correlations of compounds **2** and **3**.

Compound **2** was obtained as colorless oil. Its molecular formula was assigned to be $C_{17}H_{22}O_7$ according to the sodium adduct ionic peak at *m*/*z* 361.1226 $[M + Na]^+$, suggesting seven degrees of unsaturation. Four methyls [δ_H 1.01 (d, *J* = 6.5 Hz, 11-Me), 1.17 (d, *J* = 6.8 Hz, 12-Me), 1.21 (d, *J* = 7.0 Hz, 18-Me), and 1.93 (s, 13-Me)] and four methines [δ_H 2.52 (m, H-4), 3.82 (qd, *J* = 6.6 Hz, 1.5 Hz, H-3), 4.11 (m, H-17), and 5.08 (d, *J* = 9.7 Hz, H-1)] were recognized in the ^{1}H NMR spectrum. The ^{13}C NMR spectrum in association with the HSQC spectrum indicated 17 carbon signals ascribed to four methyls at δ_C 9.5 (q, 13-Me), 18.2 (q, 11-Me), 19.2 (q, 18-Me), and 20.1 (q, 12-Me); one methylene at δ_C 43.1 (t, C-13); four methines at δ_C 35.1 (d, C-4), 64.8 (d, C-1), 71.7 (d, C-3), and 72.2 (d, C-17); and eight nonprotonated carbons at δ_C 101.8 (s,C-7), 109.5 (s, C-5), 110.7 (s, C-9), 139.7 (s, C-10), 155.8 (s, C-8), 158.5 (s, C-6), 175.6 (s, C-14), and 211.9 (s, C-16)] .

The spin systems of 11-Me/H-3/H-4/12-Me, H-17/18-Me, and H-1/H-15 were observed in the COSY spectrum, constructing three segments (Figure 3). In the HMBC spectrum, correlations were found of 13-Me to C-5/C-6/C-10, 6-OH to C-5/C-6/C-7, 8-OH to C-7/C-8/C-9, H-4 to C-3/C-5/C-10/C-12, H-1 to C-9/C-10/C-15/C-16, H-3 to C-1, and 18-Me to C-16/C-17. Taking together the COSY and HMBC correlations, the planar structure of compound **2** was then constructed as 3-hydroxy-2-butonyldihydrocitrinin, an isomer of **1**. The relative configuration of **1** was regarded as the same with that of **2** on the basis of the key NOESY correlations of H-1/11-Me, H-3/12-Me, and H-4/11-Me (Figure 3). By the biosynthetic consideration, the absolute configuration of C-1, C-3, and C-4 in **2** and **1** should be the same. However, the stereochemistry of C-17 could not be determined. Therefore, the theoretical calculation of ECD spectrum was performed. As a result, the experimental ECD spectrum matched well with that of (1*R*,3*R*,4*S*,17*R*)-**2** (Figure 4). Consequently, the structure of **2** was assigned to be (1*R*,3*R*,4*S*,17*R*)-3-hydroxy-2-butonyldihydrocitrinin, and named penidihydrocitrinin B.

Compound **3** was isolated as colorless oils. The molecular formula of $C_{17}H_{22}O_7$ was established based on its HRESIMS data (*m*/*z* 337.1327 $[M - H]^-$, calcd for $C_{17}H_{21}O_7$, 337.1287). Its ^{1}H and ^{13}C NMR spectroscopic data were very similar to those of **2**, except for the upshift of H-17 from δ_H 4.11 to δ_H 4.02 and H_3-18 from δ_H 1.21 to 1.15, and the downshift of C-17 from δ_C 72.2 to 72.8. This implied that compound **3** could be an epimer of **2** with *S*-configuration at the C-17 position. The assumption was evidenced by the positive cotton effect (CE) at λmax 287 nm ($\Delta\varepsilon$ +0.54) in **3**, whereas a negative CE ($\Delta\varepsilon$ −0.34 at λmax 282 nm) in **2**. Final confirmation was obtained by comparison of the calculated and experimental ECD spectrum of **3**, showing the calculated ECD spectrum of (1*R*,3*R*,4*S*,17*S*)-**3** was in good accordance with that of the experimental curve (Figure 4). Accordingly, compound **3** was defined as (1*R*,3*R*,4*S*,17*S*)-3-hydroxy-2-butonyldihydrocitrinin, and named penidihydrocitrinin C.

Preprints (www.preprints.org) | NOT PEER-REVIEWED | Posted: 25 September 2023 doi:10.20944/preprints202309.1663.v1

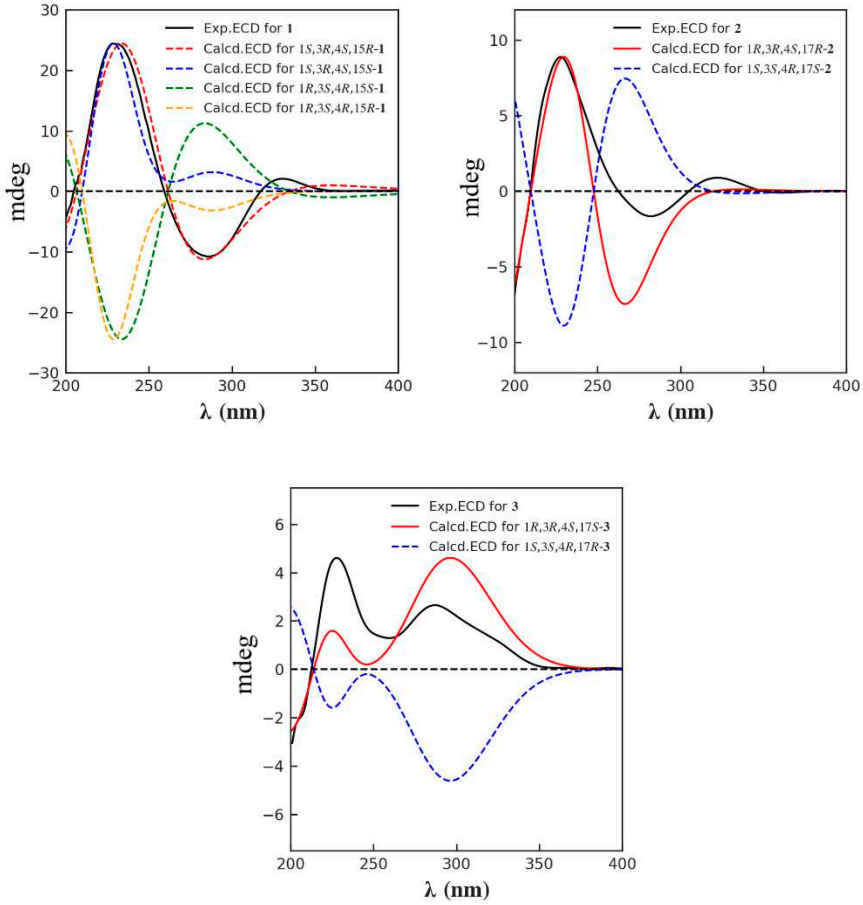

Figure 4. The calculated and experimental ECD spectra of compounds **1**–**3**.

By comparison of the NMR and MS data with those published in the literatures, 14 known compounds were identified as decarboxydihydrocitrinin (**4**) [21], dihydrocitrinin (**5**) [22], (3*R**,4*S**)-6,8-dihydroxy-3,4,7-trimethylisocoumarin (**6**) [23], sclerotinin C (**7**) [24], asperbiphenyl (**8**) [25], phenol A (**9**) [23], citrinin H2 (**10**) [26], citrinin (**11**) [27], emodin (**12**) [28], pinselin (**13**) [29], GKK1032 B (**14**) [30], neocyclocitrinol C (**15**) [31], (*Z*,*Z*)-9,12-ocadecadienoic acid methyl ester (**16**) [32], and 2,3-butanediol (**17**) [33].

Microglial activation plays a pivotal role in the pathogenesis of neurodegenerative diseases, orchestrating a complex interplay between inflammation and neuronal health [34]. While microglial cells function as the guardians of the central nervous system, their dysregulated activation can lead to chronic neuroinflammation and exacerbation of neuronal damage, contributing to the progression of disorders such as multiple sclerosis, Alzheimer's and Parkinson's diseases [35]. These diseases pose significant challenges to public health, which necessitate innovative therapeutic approaches. Thus, discovering new small molecules that can inhibit the dysregulated activation of microglia cells is essential for the targeted modulation of the immune response in the central nervous system, which can reduce inflammation and protect neurons from harm [36]. A growing number of evidences demonstrate that secondary metabolites derived from marine resources are potential therapeutic strategies for microglial-mediated neuroinflammation.

Therefore, all isolates were tested for nitrite secretion in lipopolysaccharide (LPS)-induced BV-2 microglial cells. As a result, they all demonstrated a dose-dependent suppression of nitrite secretion induced by LPS, displaying inhibitory actions at concentrations between 20 to 3 μM (Figure 5). Moreover, none exhibited cytotoxicity effects against BV-2 cells at 20 μM under the microscope. We further compared the inhibition of these compounds on nitrite production at a concentration of 10 μM (Figure 6), and the results showed that the inhibitory rates of compounds **1**–**7** on nitrite production were between 31.1%–53.5% which indicates that substitution of the C-1 position on

Preprints (www.preprints.org) | NOT PEER-REVIEWED | Posted: 25 September 2023 doi:10.20944/preprints202309.1663.v1

isochroman weakened the anti-inflammatory activity of the compounds, suggesting that this substitution is related to anti-inflammatory activity. Compound **8** only inhibite 26.4% nitrite production in LPS stimulated BV-2 cell, demonstrating that dimer structure further weakened the anti-inflammatory effect. Notably, compound **14** (GKK1032 B) displayed the most potent nitrite inhibitory activity with an inhibitory ratio of 73.0±1.6% at 10 μM (nitrite concentration: 12.2±0.4 μM), compared to LPS treated group (nitrite concentration: 30.9 ± 0.4 μM) (Figures 5 and 6). Furthermore, this compound displayed an IC_{50} value of 4.7 μM. Although GKK1032 analogues were reported to exhibit antibacterial activities [37], it is the first time that it had anti-neuroinflammatory activity. These findings demonstrate the effects of marine-derived compounds in modulating microglial activation, suggesting their potential as therapeutic candidates for neuroinflammatory conditions and neurodegenerative diseases.

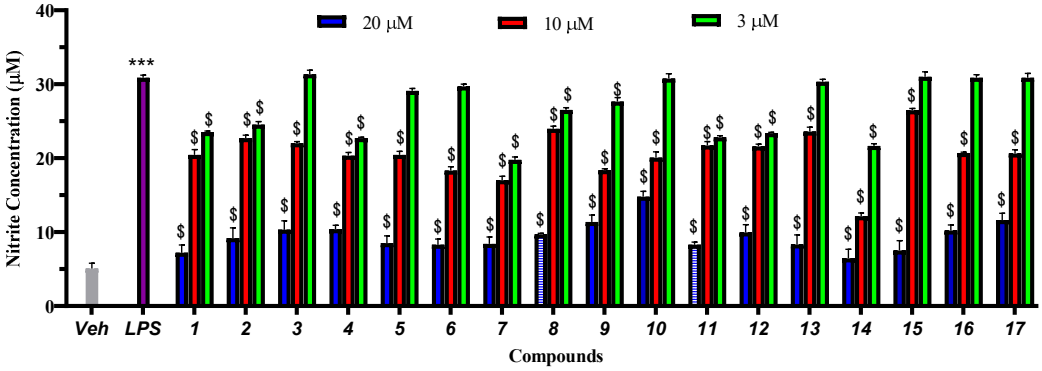

Figure 5. Effects of compounds **1–17** against nitrite production in LPS induced BV-2 cells. ***, Veh *vs* LPS, p<0.0001. $, Compounds *vs* LPS, p<0.0001.

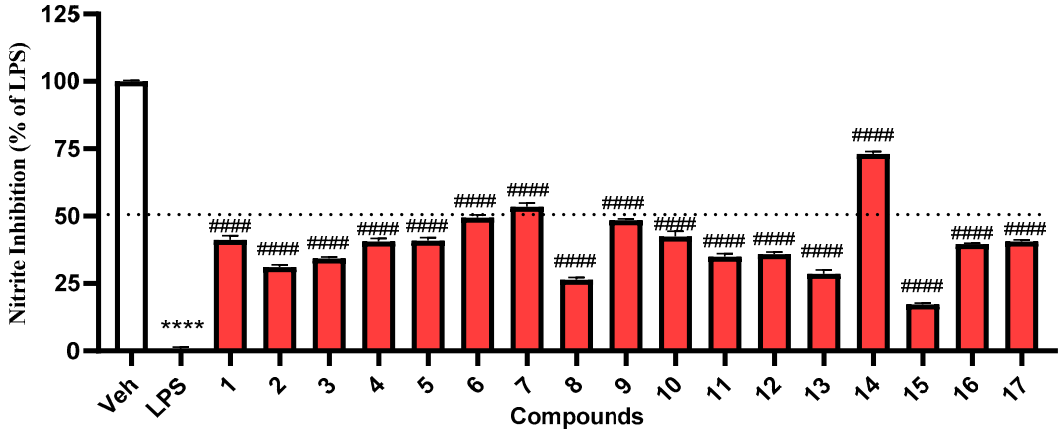

Figure 6. Effects of compounds **1–17** inhibition nitrite production in LPS induced BV-2 cells at 10 μM. ****, Veh *vs* LPS, p<0.0001. ####, Compounds *vs* LPS, p<0.0001.

Osteoporosis, a disease associated with aging, is characterized by excessive activation of osteoclasts or reduction of osteoblasts. Among women aged 65 or older, approximately 25% are affected by osteoporosis, with accelerated bone loss occurring after menopause. Therefore, promoting osteoblast differentiation and suppressing osteoclastogenesis are effective strategies for treating osteoporosis [38]. BMSCs are able to differentiate into osteoblasts, chondroblasts, and adipocytes [39], and bone regeneration achieved via osteogenic induction of MSCs could provide a rational therapeutic strategy for preventing age-related osteoporosis [40]. In this study, all 17 isolates were

Preprints (www.preprints.org) | NOT PEER-REVIEWED | Posted: 25 September 2023 doi:10.20944/preprints202309.1663.v1

tested for both osteoblast and osteoclast activity. At a concentration of 10 μM, all the compounds had no cytotoxic effect on BMSCs (Figure 7).

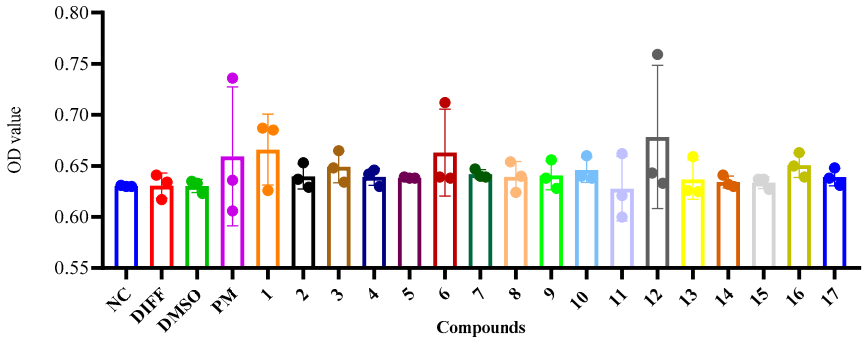

Figure 7. BMSCs viability was measured by the CCK-8 assay.

Intracellular calcium deposition at a later stage served as a significant evaluation indicator for osteogenic activity. Interestingly, compounds **6**, **7**, and **8** exerted a noticeable enhancing effect on osteoblast mineralization within BMSCs (Figure 8).

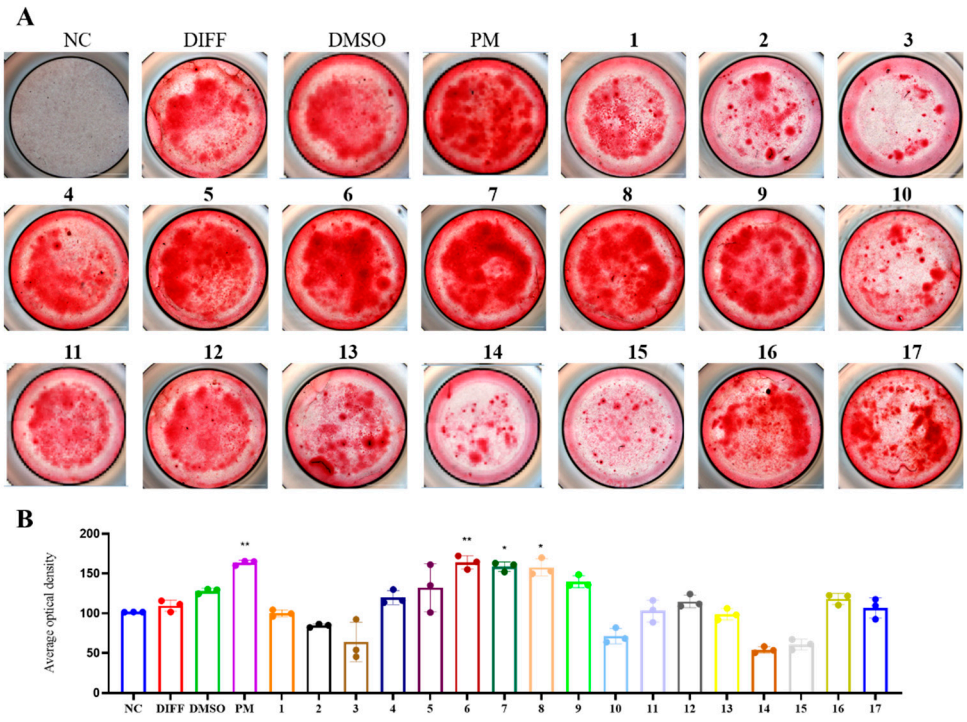

Figure 8. Preliminary screening results for the ability of compounds **1**–**17** to induce osteoblast activity among BMSCs. (A) Alizarin Red S staining. The BMSCs were cultures exposed to compounds **1**–**17** with osteogenic inducer. After 14 days, the cells were stained with alizarin red S and take pictures by Biotek cytation-5. The culture medium, osteogenesis differentiation medium (50 μg/mL ascorbic acid and 5 mM β-glycerophosphate), DMSO (0.1%), and purmorphamine (1 μM) were regarded as the negative control (NC), differentiation (DIFF), solvent (DMSO), and positive control groups (PM), respectively. Scar bar=1000 μM (B) Quantification of Alizarin Red S staining based on average optical density. *p<0.05, ** p <0.01 *vs* the DMSO group.

Furthermore, bioactive compounds **6**, **7**, and **8** also exhibited a distinct inhibitory effect on osteoclast activity, as evidenced by a significant reduction in tartrate-resistant acid phosphatase

Preprints (www.preprints.org) | NOT PEER-REVIEWED | Posted: 25 September 2023 doi:10.20944/preprints202309.1663.v1

(TRAP) positive cells (Figure 9). These findings indicate that compounds **6**, **7**, and **8** not only facilitated osteoblast mineralization but also exerted a substantial dose-dependent inhibitory effect on RANKL-induced osteoclasts.

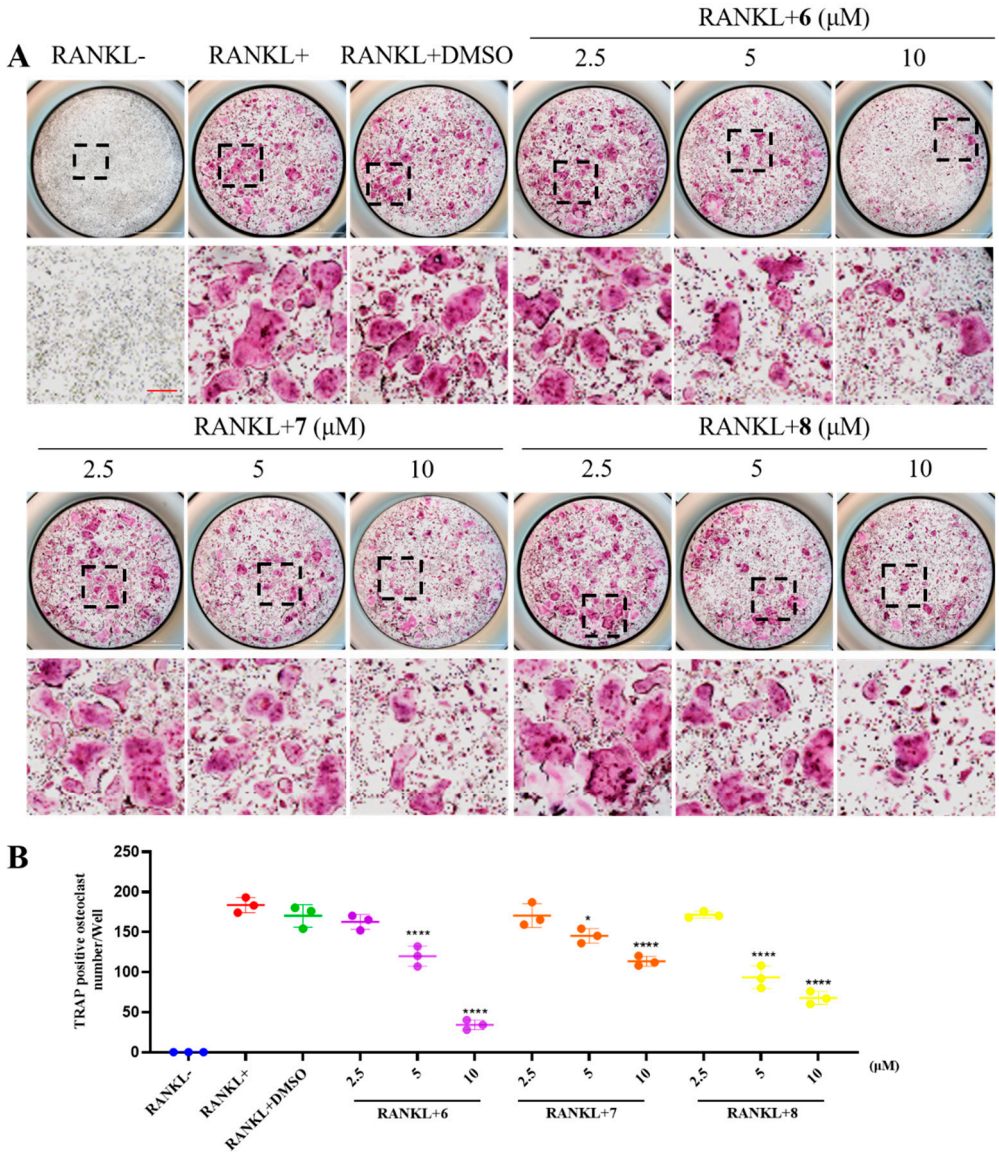

Figure 9. Compound **6**, **7**, and **8** attenuated RANKL-activated osteoclastogenesis by dose-dependently. BMMs cultured with 0, 2.5, 5, or 10 μM compounds with the stimulation of 25 ng/ml RANKL (or not). After five days, these cells were fixed and stained with TRAP. (B) TRAP-positive multinucleated (there or more) cells were regarded as mature osteoclasts. Osteoclast number were quantified and analyzed (n = 3). *p<0.05, ** p <0.01, *** p <0.001 *vs* the DMSO group.

3. Materials and Methods

3.1. General Experimental Procedures

NMR spectra of all compounds were recorded on a Bruker 400 MHz spectrometer (Bruker, Fällanden, Switzerland). Optical rotations were measured by an Anton Paar polarimeter (MCP100). The high-resolution electrospray-ionisation mass spectrometry (HRESIMS) were acquired on a Xevo G2 Q-TOF mass spectrometer (Waters). ECD spectra were measured on a Chirascan spectrometer. The semi-preparative HPLC was performed on an Agilent instrument (1260) with a semi-preparative

chromatographic column (COSMOSIL 5 C18-MS-II, Nacalai Tesque, Japan). Column chromatography (CC) was performed on silica gel, Sephadex LH-20, and octadecyl silyl (ODS).

3.2. Fungal Identification, Fermentation, and Extraction

The fungal strain W17 was isolated from a deep-sea sediment sample of the Western Pacific Ocean at the depth of 5278 m. It was identified to be *Penicillium citrinum* as the 18S rRNA gene sequence alignment (OR398934) demonstrated that it showed great similarity (99.8%) to *Penicillium citrinum* NRRL 1841 (GenBank accession number NR_121224.1). The strain was preserved at Key Laboratory of Marine Genetic Resources, Third Institute of Oceanography, Ministry of Natural Resources (Xiamen, China). The microbial strain was cultivated on a PDA plate medium at 25 °C for 3 days and the colony was inoculated into 250 mL Erlenmeyer flasks containing 50 mL PDB medium. Then it was cultured in a rotary shaker (130 rpm) at 25 °C for 3 days as the spores' medium. After 3 days, the spores' solution was inoculated in 120 Erlenmeyer flasks (1 L) with each containing 400 mL tap water, 80 g potato power, 8 g glucose, and 6 g marine salt. The fermentation was performed in a 130 rpm rotary shaker at 25 °C. After 7 days, the fermentation broth was extracted with EtOAc three times and concentrated under reduced pressure to give a crude extract (36.5 g).

3.3. Isolation and Purification

The crude extract (36.5 g) was separated into seven fractions (Fr.1−Fr.7) *via* column chromatography (CC) over silica gel using gradient CH_2Cl_2-MeOH (100%→75%). Fraction Fr.4 (3.6 g) were subsequently separated by CC over ODS (octadecyl silyl) (MeOH-H_2O, 5%→100%), Sephadex LH-20 (MeOH), and semi-preparative HPLC with MeOH-H_2O (40%→100%) to yield **1** (5.7 mg) and **4** (15.4 mg). Fraction Fr.7 (1.5 g) was separated by CC over Sephadex LH-20 (MeOH), silica gel (CH_2Cl_2-MeOH, 10:1), and semi-preparative HPLC with MeOH-H_2O (30%→60%) to yield **2** (1 mg), **3** (1 mg), and **6** (45.9 mg). Compound **11** (43 mg) was purified from Fr.1 (5 g) by recrystallization in MeOH, while compounds **14** (14 mg) and **16** (49 mg) were isolated by CC over ODS (50%→100%), Sephadex LH-20 (MeOH), and Prep.TLC (CH_2Cl_2-MeOH, 50:1). Fraction Fr.2 (2.0 g) was subjected to ODS (10%→100%) and Sephadex LH-20 (MeOH) to yield compound **12** (69 mg). Fraction Fr.3 was subjected to CC on ODS (10%→100%) and Sephadex LH-20 (MeOH). Final purification by semi-prep. HPLC (MeOH-H_2O, 60%→90%) afforded **9** (1.6 mg) and **10** (3.7 mg). Fraction Fr.5 (4.6 g) was separated by CC over ODS (10%→100%), Sephadex LH-20 (MeOH), and semi-prep. HPLC (MeOH-H_2O, 30%→60%) to give **5** (124 mg), **13** (7 mg), **15** (2.1 mg), and **17** (190 mg). Compounds **7** (15.2 mg) and **8** (22.4 mg) were obtained by CC over ODS (10%→100%), Sephadex LH-20 (MeOH), and semi-prep. HPLC (MeOH-H_2O, 30%→60%) from Fr.6 (2.0 g).

Penidihydrocitrinin A (**1**): yellow amorphous powder; $[\alpha]_D^{25}$ +28.0 (*c* 0.10, MeOH); UV (MeOH) λmax (logε) 214 (3.16), 244 (2.64), 252 (2.65), 280 (1.85), 319 (2.16) nm; CD (MeOH) ($\Delta\varepsilon$) 229 (+5.00), 233 (+0.53), 286 (−2.20), 330 (+0.42) nm; ^{1}H and ^{13}C NMR data, see Table 1; HRESIMS *m*/*z* 337.1309 $[M - H]^-$ (calcd for $C_{17}H_{21}O_7$ 337.1287).

Penidihydrocitrinin B (**2**): colorless oil; $[\alpha]_D^{25}$ +25.0 (*c* 0.10, MeOH); UV (MeOH) λmax (logε) 204 (2.78), 214 (2.84), 242 (2.28), 253 (2.32), 276 (1.40), 319 (1.90) nm; CD (MeOH) ($\Delta\varepsilon$) 228 (+1.82), 282 (−0.34), 322 (+0.18) nm; ^{1}H and ^{13}C NMR data, see Table 1; HRESIMS *m*/*z* 361.1226 $[M + Na]^+$ (calcd for $C_{17}H_{22}O_7Na$ 361.1263).

Penidihydrocitrinin C (**3**): colorless oil; $[\alpha]_D^{25}$ +40.0 (*c* 0.10, MeOH); UV (MeOH) λmax (logε) 205 (2.71), 213 (2.72), 253 (2.24), 275 (1.39), 320 (1.83) nm; CD (MeOH) ($\Delta\varepsilon$) 228 (+0.94), 260 (+0.26), 287 (+0.54) nm; ^{1}H and ^{13}C NMR data, see Table 1; HRESIMS *m*/*z* 337.1327 $[M - H]^-$ (calcd for $C_{17}H_{21}O_7$, 337.1287).

3.4. ECD Calculation

As reported previously [18], the conformational analysis was first conducted *via* random searching in the Stochastic using the MMFF94 force field. All conformers were consecutively optimized at the PM6 and HF/6-31G(d)levels. Dominative conformers were further optimized at the

 doi:10.20944/preprints202309.1663.v1

B3LYP/6-31G(d) level in the gas phase. The optimized conformers possessed no imaginary frequencies and were true local minima. ECD calculations were conducted at B3LYP/6-311G(d,p) level in MeOH with IEFPCM model using Time-dependent Density Functional Theory (TD-DFT). The ECD spectrum was simulated by overlapping Gaussian functions for each transition.

3.5. BV-2 Cell Culture and Compounds Treatment

BV-2 cell culture and compounds treatment as previously reported [41,42]. Briefly, BV-2 microglia cells were cultured in DMEM medium supplemented with 10% fetal bovine serum (Thermofisher, Shanghai, China) and antibiotics (100 units/mL of penicillin and 100 μg/mL of streptomycin) in a humidified 5% CO_2 incubator at 37°C. Cells were seeded into 24-well plates at a density of 2×10^4 cells per well and allowed to adhere overnight. On the subsequent day, the cells were treated with freshly prepared culture medium containing the specified concentrations of the investigated compounds for a duration of 30 minutes before exposure to LPS (1 μg/mL). A control group was treated with a vehicle solution (DMSO, 0.1%).

3.6. Quantification of Nitrite Levels

The concentration of nitrite present in the culture medium was assessed using the Griess Reagent Kit (Thermo Fisher, Shanghai, China). Briefly, 75 μL of cell culture supernatants were mixed with an equal volume of the Griess Reagent Kit and allowed to react for 30 minutes at room temperature. The absorbance of the resulting diazonium compound was measured at a wavelength of 560 nm. The concentration of nitrite production was calculated based on the nitrite standard solution.

3.7. Cell Extraction and Culture

The bone mesenchymal stem cells (BMSCs) and bone marrow monocytes (BMMs) were flushed from the femur of C57BL/6J mice aged 3 weeks and 6-week-old C57BL/6 mice, respectively, with the methods as previously described [16]. In brief, the BMSCs was carefully removed from animal and cultured in α-MEM and induced with supplemented complete α-MEM medium (10% vol/vol FBS, 1% vol/vol penicillin/streptomycin [P/S]). The BMSCs was induced with 2 mM β-glycerophosphate and 50 μg/mL ascorbate, of which half were changed twice a week. The BMMs cultured in complete α-MEM medium (10% vol/vol FBS, 1% vol/vol P/S, and 50 ng/mL M-CSF).

3.8. CCK-8 Assay

The *in vitro* cytotoxic bioassay was conducted using the CCK-8 method according to the previously reported protocols [16]. The BMSCs were treated with or without compounds. After 48 h of culture, cells were treated with CCK-8 solution for 2 h before being scanned with a multimode scanner at 450 nm (Biotek, United States).

3.9. Osteoblast Differentiation and Mineralization

The BMSCs were digested and planted at a density of 2×10^4 cells/well into 96-well plates and cultivated overnight. Ascorbic acid (50 μg/mL) and β-glycerophosphate (5 mM) were added into the culture medium for osteogenic assay. The culture medium was changed every other day. ALP activity was performed after 7 days of differentiation, and AR staining was performed after 14 days of differentiation. For ALP activity, the cells were incubated with 10-fold diluted alamar blue solutions for 4 h, and washed for 3 times. The cells were incubated with a solution containing phosphatase substratenitrophenol phosphate (pNPP), 6.5 mM Na_2CO_3, 18.5 mM $NaHCO_3$, 2 mM $MgCl_2$ (Sigma-Aldrich). The alkaline phosphatase (ALP) activity was assessed using pNPP as the substrate at pH 10.2 by evaluating the optical density of the yellow substance at 405 nm. Alizarin red staining was used to check the calcification conditions in cultures. Fixed cells with 10 % neutral-buffered formalin for 30 min and next 2% Alizarin red S was used to incubate cells for 2 min at room temperature. Then the cells were taken pictures by Biotek cytation-5.

3.10. Osteoclast Differentiation

BMMs were cultured for 7 days in the presence of M-CSF (25 ng/mL) and RANKL (25 ng/mL) for differentiation into mature osteoclasts. Media was refreshed every 2 days. For tartrate-resistant acid phosphatase (TRAP) staining, cells were fixed with 4 % paraformaldehyde (PFA) and stained for TRAP activity. Under a microscope (Biotek cytation-5, USA), TRAP-positive multi-nucleated cells with three nuclei were counted as osteoclasts.

4. Conclusions

In summary, three new polyketides (penidihydrocitrinins A–C, **1–3**) were isolated from the deep-sea-derived *Penicillium citrinum* W17 together with 14 known compounds (**4–17**). Compound **14** displayed the most potent inhibitory activity in LPS-induced BV-2 cell model with an IC_{50} value of 4.7 μM. While compounds **6**, **7**, and **8** not only promoted the osteoblasts mineralization, but also had a significant inhibitory effect on RANKL-induced osteoclasts. These findings not only enriched the structural diversity of polyketides, but also provided potential molecules for anti-inflammatory and anti-osteoporotic activity.

Supplementary Materials: The following supporting information can be downloaded at the website of this paper posted on Preprints.org, Figures S1–S21: One-dimensional and two-dimensional NMR spectra along with HR-ESI-MS spectra of compounds **1–3**.

Author Contributions: X.-W.Y. designed the project; Y.Z. and Z.-B.Z. isolated and purified all compounds. C.-L.X. and R.X. conducted the anti-osteoporotic experiments; X.-W.H. and L.-H.Y. performed the anti-inflammatory bioassay. K.Z. identified the strain. Y.L., and M.-M.X. performed the fermentation. Y.Z., Y.W., and X.-W.Y. analyzed the data and wrote the paper, while critical revision of the publication was performed by all authors. All authors have read and agreed to the published version of the manuscript.

Funding: The work was supported by the National Key Research and Development Program of China (2022YFC2804800), the Xiamen Southern Oceanographic Center (22GYY007HJ07), and the National Natural Science Foundation of China (22177143).

Institutional Review Board Statement: Not applicable.

Informed Consent Statement: Not applicable.

Acknowledgments: The authors wish to thank Xiao-Yong Zhang of South China Agricultural University to isolate the fungal strain.

Conflicts of Interest: The authors declare no conflict of interest.

References

1. Carroll, A. R.; Copp, B. R.; Davis, R. A.; Keyzers, R. A.; Prinsep, M. R. Marine natural products. *Nat. Prod. Rep.* **2023**, *40*, 275-325.
2. Voser, T. M.; Campbell, M. D.; Carroll, A. R. How different are marine microbial natural products compared to their terrestrial counterparts? *Nat. Prod. Rep.* **2022**, *39*, 7-19.
3. Carroll, A. R.; Copp, B. R.; Davis, R. A.; Keyzers, R. A.; Prinsep, M. R. Marine natural products. *Nat. Prod. Rep.* **2022**, *39*, 1122-1171.
4. Skropeta, D.; Wei, L. Recent advances in deep-sea natural products. *Nat. Prod. Rep.* **2014**, *31*, 999-1025.
5. Sun, C.; Mudassir, S.; Zhang, Z.; Feng, Y.; Chang, Y.; Che, Q.; Gu, Q.; Zhu, T.; Zhang, G.; Li, D. Secondary metabolites from deep-sea derived microorganisms. *Curr. Med. Chem.* **2020**, *27*, 6244-6273.
6. Chooi, Y. H.; Tang, Y. Navigating the fungal polyketide chemical space: from genes to molecules. *J. Org. Chem.* **2012**, *77*, 9933-9953.
7. Niu, S.; Tang, X. X.; Fan, Z.; Xia, J. M.; Xie, C. L.; Yang, X. W. Fusarisolins A-E, polyketides from the marine-derived fungus *Fusarium solani* H918. *Mar. Drugs* **2019**, *17*, 125.
8. Pojer, F.; Ferrer, J. L.; Richard, S. B.; Nagegowda, D. A.; Chye, M. L.; Bach, T. J.; Noel, J. P. Structural basis for the design of potent and species-specific inhibitors of 3-hydroxy-3-methylglutaryl CoA synthases. *Proc. Natl. Acad. Sci. USA* **2006**, *103*, 11491-11496.

9. De Pascale, G.; Nazi, I.; Harrison, P. H.; Wright, G. D. β-Lactone natural products and derivatives inactivate homoserine transacetylase, a target for antimicrobial agents. *J. Antibiot.* **2011**, *64*, 483-487.
10. Feling, R. H.; Buchanan, G. O.; Mincer, T. J.; Kauffman, C. A.; Jensen, P. R.; Fenical, W. Salinosporamide A: A highly cytotoxic proteasome inhibitor from a novel microbial source, a marine bacterium of the new genus *salinospora*. *Angew. Chem. Int. Ed.* **2003**, *42*, 355-357.
11. Liu, Y. F.; Zhang, Y. H.; Shao, C. L.; Cao, F.; Wang, C. Y. Microketides A and B, polyketides from a gorgonian-derived *Microsphaeropsis* sp. fungus. *J. Nat. Prod.* **2020**, *83*, 1300-1304.
12. Hsieh, M. H.; Hsiao, G.; Chang, C. H.; Yang, Y. L.; Ju, Y. M.; Kuo, Y. H.; Lee, T. H. Polyketides with anti-neuroinflammatory activity from *Theissenia cinerea*. *J. Nat. Prod.* **2021**, *84*, 1898-1903.
13. Chen, M.; Zheng, Y. Y.; Chen, Z. Q.; Shen, N. X.; Shen, L.; Zhang, F. M.; Zhou, X. J.; Wang, C. Y. NaBr-induced production of brominated azaphilones and related tricyclic polyketides by the marine-derived fungus *Penicillium janthinellum* HK1-6. *J. Nat. Prod.* **2019**, *82*, 368-374.
14. Liu, Y.; Yang, Q.; Xia, G.; Huang, H.; Li, H.; Ma, L.; Lu, Y.; He, L.; Xia, X.; She, Z. Polyketides with α-glucosidase inhibitory activity from a mangrove endophytic fungus, *Penicillium* sp. HN29-3B1. *J. Nat. Prod.* **2015**, *78*, 1816-1822.
15. Li, D.; Chen, L.; Zhu, T.; Kurtán, T.; Mándi, A.; Zhao, Z.; Li, J.; Gu, Q. Chloctanspirones A and B, novel chlorinated polyketides with an unprecedented skeleton, from marine sediment derived fungus *Penicillium terrestre*. *Tetrahedron* **2011**, *67*, 7913-7918.
16. He, Z. H.; Xie, C. L.; Wu, T.; Yue, Y. T.; Wang, C. F.; Xu, L.; Xie, M. M.; Zhang, Y.; Hao, Y. J.; Xu, R.; Yang, X. W. Tetracyclic steroids bearing a bicyclo[4.4.1] ring system as potent antiosteoporosis agents from the deep-sea-derived fungus *Rhizopus* sp. W23. *J. Nat. Prod.* **2023**, *86*, 157-165.
17. Hao, Y. J.; Zou, Z. B.; Xie, M. M.; Zhang, Y.; Xu, L.; Yu, H. Y.; Ma, H. B.; Yang, X. W. Ferroptosis inhibitory compounds from the deep-sea-derived fungus *Penicillium* sp. MCCC 3A00126. *Mar. Drugs* **2023**, *21*, 234.
18. He, Z. H.; Xie, C. L.; Wu, T.; Zhang, Y.; Zou, Z. B.; Xie, M. M.; Xu, L.; Capon, R. J.; Xu, R.; Yang, X. W. Neotricitrinols A-C, unprecedented citrinin trimers with anti-osteoporosis activity from the deep-sea-derived *Penicillium citrinum* W23. *Bioorg. Chem.* **2023**, *139*, 106756.
19. Xie, C. L.; Zhang, D.; Guo, K. Q.; Yan, Q. X.; Zou, Z. B.; He, Z. H.; Wu, Z.; Zhang, X. K.; Chen, H. F.; Yang, X. W. Meroterpenthiazole A, a unique meroterpenoid from the deep-sea-derived *Penicillium allii-sativi*, significantly inhibited retinoid X receptor (RXR)-α transcriptional effect. *Chin. Chem. Lett.* **2022**, *33*, 2057-2059.
20. Niu, S.; Xie, C. L.; Xia, J. M.; Liu, Q. M.; Peng, G.; Liu, G. M.; Yang, X. W. Botryotins A–H, tetracyclic diterpenoids representing three carbon skeletons from a deep-sea-derived *Botryotinia fuckeliana*. *Org. Lett.* **2020**, *22*, 580-583.
21. Wakana, D.; Hosoe, T.; Itabashi, T.; Okada, K.; de Campos Takaki, G. M.; Yaguchi, T.; Fukushima, K.; Kawai, K. New citrinin derivatives isolated from *Penicillium citrinum*. *J. Nat. Med.* **2006**, *60*, 279-284.
22. Deruiter, J.; Jacyno, J. M.; Davis, R. A.; Cutler, H. G. Studies on aldose reductase inhibitors from fungi. I. Citrinin and related benzopyran derivatives. *J. Enzyme. Inhib.* **1992**, *6*, 201-210.
23. Han, Z.; Mei, W.; Zhao, Y.; Deng, Y.; Dai, H. A new cytotoxic isocoumarin from endophytic fungus *Penicillium* SP. 091402 of the mangrove plant *Bruguiera sexangula*. *Chem. Nat. Compd.* **2010**, *45*, 805-807.
24. Kuramata, M.; Fujioka, S.; Shimada, A.; Kawano, T.; Kimura, Y. Citrinolactones A, B and C, and sclerotinin C, plant growth regulators from *Penicillium citrinum*. *Biosci. Biotechnol. Biochem.* **2007**, *71*, 499-503.
25. Wu, Z. J.; Ouyang, M. A.; Tan, Q. W. New asperxanthone and asperbiphenyl from the marine fungus *Aspergillus* sp. *Pest. Manag. Sci.* **2009**, *65*, 60-65.
26. Hirota, M.; Menta, A. B.; Yoneyama, K.; and Kitabatake, N. A major decomposition product, citrinin H2, from citrinin on heating with moisture. *Biosci. Biotechnol. Biochem.* **2002**, *66*, 206-210.
27. Chai, Y. J.; Cui, C. B.; Li, C. W.; Wu, C. J.; Tian, C. K.; Hua, W. Activation of the dormant secondary metabolite production by introducing gentamicin-resistance in a marine-derived *Penicillium purpurogenum* G59. *Mar. Drugs* **2012**, *10*, 559-582.
28. Li, S. F.; Di, Y. T.; Wang, Y. H.; Tan, C. J.; Fang, X.; Zhang, Y.; Zheng, Y. T.; Li, L.; He, H. P.; Li, S. L.; Hao, X. J. Anthraquinones and Lignans from *Cassia occidentalis*. *Helv. Chim. Acta* **2010**, *93*, 1795-1802.
29. Kim, S.; Le, T. C.; Han, S. A.; Hillman, P. F.; Hong, A.; Hwang, S.; Du, Y. E.; Kim, H.; Oh, D. C.; Cha, S. S.; Lee, J.; Nam, S. J.; Fenical, W. Saccharobisindole, neoasterric methyl ester, and 7-chloro-4(1H)-quinolone: three new compounds isolated from the marine bacterium *Saccharomonospora* sp. *Mar. Drugs* **2021**, *20*, 35.

30. Oilawa, H. Biosynthesis of structurally unique fungal metabolite GKK1032A2: indication of novel carbocyclic formation mechanism in polyketide biosynthesis. *J. Org. Chem.* **2003**, *68*, 3552-3557.
31. Ren, J. M.; Yang, J. K.; Zhu, H. J.; Cao, F. Bioactive steroids from the marine-derived fungus *Aspergillus flavus* JK07-1. *Chem. Nat. Compd.* **2020**, *56*, 945-947.
32. Biswas, A.; Sharma, B. K.; Willett, J. L.; Erhan, S. Z.; Cheng, H. N. Room-temperature self-curing ene reactions involving soybean oil. *Green Chem.* **2008**, *10*, 290-295.
33. Uemura, Y.; Sugimoto, S.; Matsunami, K.; Otsuka, H.; Takeda, Y.; Kawahata, M.; Yamaguchi, K. Microtropins A-I: 6'-*O*-(2''*S*,3''*R*)-2''-ethyl-2'',3''-dihydroxybutyrates of aliphatic alcohol *β*-D-glucopyranosides from the branches of *Microtropis japonica*. *Phytochemistry* **2013**, *87*, 140-147.
34. Dheen, S. T.; Kaur, C.; Ling, E. A. Microglial activation and its implications in the brain diseases. *Curr. Med. Chem.* **2007**, *14*, 1189-1197.
35. Rawji, K. S.; Mishra, M. K.; Michaels, N. J.; Rivest, S.; Stys, P. K.; Yong, V. W. Immunosenescence of microglia and macrophages: impact on the ageing central nervous system. *Brain* **2016**, *139*, 653-661.
36. Costa, T.; Fernandez-Villalba, E.; Izura, V.; Lucas-Ochoa, A. M.; Menezes-Filho, N. J.; Santana, R. C.; de Oliveira, M. D.; Araujo, F. M.; Estrada, C.; Silva, V.; Costa, S. L.; Herrero, M. T. Combined 1-deoxynojirimycin and ibuprofen treatment decreases microglial activation, phagocytosis and dopaminergic degeneration in MPTP-treated mice. *J. Neuroimmune Pharmacol.* **2021**, *16*, 390-402.
37. Song, T.; Chen, M.; Ge, Z. W.; Chai, W.; Li, X. C.; Zhang, Z.; Lian, X. Y. Bioactive penicipyrrodiether A, an adduct of GKK1032 analogue and phenol A derivative, from a marine-sourced fungus *Penicillium* sp. ZZ380. *J. Org. Chem.* **2018**, *83*, 13395-13401.
38. El-Desoky, A. H. H.; Tsukamoto, S. Marine natural products that inhibit osteoclastogenesis and promote osteoblast differentiation. *J. Nat. Med.* **2022**, *76*, 575-583.
39. Sun, Y.; Li, Q. F.; Yan, J.; Hu, R.; Jiang, H. Isoflurane preconditioning promotes the survival and migration of bone marrow stromal cells. *Cell Physiol. Biochem.* **2015**, *36*, 1331-1345.
40. Guan, M.; Yao, W.; Liu, R.; Lam, K. S.; Nolta, J.; Jia, J.; Panganiban, B.; Meng, L.; Zhou, P.; Shahnazari, M.; Ritchie, R. O.; Lane, N. E. Directing mesenchymal stem cells to bone to augment bone formation and increase bone mass. *Nat. Med.* **2012**, *18*, 456-462.
41. Yang, L. H.; Ou-Yang, H.; Yan, X.; Tang, B. W.; Fang, M. J.; Wu, Z.; Chen, J. W.; Qiu, Y. K. Open-ring butenolides from a marine-derived anti-neuroinflammatory fungus *Aspergillus terreus* Y10. *Mar. Drugs* **2018**, *16*, 428.
42. Niu, S.; Yang, L.; Zhang, G.; Chen, T.; Hong, B.; Pei, S.; Shao, Z. Phenolic bisabolane and cuparene sesquiterpenoids with anti-inflammatory activities from the deep-sea-derived *Aspergillus sydowii* MCCC 3A00324 fungus. *Bioorg. Chem.* **2020**, *105*, 104420.